Available online at www.sciencedirect.com

ScienceDirect

Procedia Manufacturing 34 (2019) 584–593

Procedia MANUFACTURING

www.elsevier.com/locate/procedia

47th SME North American Manufacturing Research Conference, Penn State Behrend Erie, Pennsylvania, 2019

Deposition Group-based Toolpath Planning for Additive Manufacturing with Multiple Robotic Actuators

Yi Cai[a,*], S.H. Choi[b]

[a]*North Carolina A&T State University, Greensboro, NC 27411, United States*

[b]*The University of Hong Kong, Hong Kong, Hong Kong*

* Corresponding author. Tel.: +1-336-285-3162; fax: +1-336-285-0000. *E-mail address:* ycai@ncat.edu

Abstract

This paper proposes a practical approach for toolpath planning of vector-based additive manufacturing (AM) processes with multiple robotic actuators. It classifies and models the operational spatial constraints of possible actuator collisions and indexes the deposition priorities of materials. The contours within each layer of a multi-material object are sorted according to material deposition priorities, material distribution on the actuators, and the spatial constraints for collision avoidance. The sorted contours are then arranged into a series of deposition groups for subsequent concurrent fabrication. The proposed approach has been incorporated into a virtual prototyping system for visualization and validation of AM processes with various types of robotic actuators. Case studies show that it can greatly improve the concurrency of material deposition, and hence reduce the build time of complex multi-material and large single-material objects substantially. It can be practically adapted for control of AM processes with multiple robotic actuators.

Keywords: Additive manufacturing; Multiple robotic actuators; Constraint modeling; Toolpath planning; Concurrent fabrication

1. Introduction

The last three decades have seen the proliferation of additive manufacturing (AM) in a wide range of fields, although most current processes can only fabricate objects of a single material. In recent years, there have been imminent demands for multi-material additive manufacturing (MMAM) processes, because an increasing proportion of objects, especially for advanced products and biomedical applications, comprise of multiple materials.

According to the fabrication principle, current AM processes can be categorized into raster-based and vector-based. In a typical raster-based AM process, a whole layer of liquid or powder material is prepared and selectively solidified by laser scanning, or by image masking, or by glue spray from ink-jet arrays. Examples include Stereolithography Apparatus (SLA), Selective Laser Sintering (SLS), and 3D Printing (3DP) [1]. Since their speed is comparatively fast, some raster-based AM processes have been adapted for experimental fabrication of discrete multi-material and functionally graded material (FGM) objects. However, this advantage is often diminished by a need for complicated material allocation and transference mechanisms to prepare material powder with varying compositions within a layer, which increases the cost and slows down the fabrication speed considerably [2-4]. Moreover, some critical problems, such as contamination of different material powders or resins, low material utilization, and difficulties in recycling from blended powders, have to be addressed.

Vector-based AM processes, on the other hand, are suitable for fabrication of multi-material objects. In such processes, one or multiple tools (usually nozzles) are driven along predefined paths to deposit fabrication materials. Fused Deposition Modeling (FDM), Laser Engineered Net Shaping (LENS), and Direct Metal Deposition (DMD) are typical of this category [5-

2351-9789 © 2019 The Authors. Published by Elsevier B.V.

10.1016/j.promfg.2019.06.223

7]. They exhibit process intuition, versatile choices of materials, and better control of material deposition and composition. Moreover, they offer high material utilization, convenient maintenance, and easy extension into MMAM systems. Indeed, many emerging experimental and commercial MMAM systems are vector-based [8-11].

Nevertheless, vector-based AM processes are relatively slow, particularly when large cross sections are involved or smaller hatch widths are required for high accuracy, because solid contours have to be filled with mere single deposition lines of material. Bellini *et al.* [12] observed that FDM is fast enough for small objects or for thin and tall structures, but takes too long to fabricate objects with large sections. For medical applications, Giannatsis and Dedoussis [13] claimed that the build times are often too long for emergency cases and hence restricts the use of AM in many situations. Wohler [14] also pointed out that the fabrication speed of the current AM systems has become unsatisfactory because of the ever-increasing complexity and size of products.

A way to improve the fabrication speed is to introduce multiple actuators for concurrent deposition of materials. Indeed, there have been attempts to employ multiple actuators for vector-based AM, although the corresponding toolpath planning technique has yet to be further developed. For FDM, Wachsmuth [15] grouped a few extrusion heads to fabricate prototypes with large cross sections. Zhang and Khoshnevis [16] introduced contour crafting using multiple nozzles for building large constructions. They presented three corresponding toolpath planning algorithms, which were basically focused on single-material objects and could not be applied for MMAM directly. Zhu and Yu [17] proposed a spatio-temporal approach to toolpath planning for small, simple multi-material assemblies. Choi and Cheung [18] proposed a topological hierarchy-based method to group the contour toolpaths within a layer into toolpath sets for concurrent deposition of different materials. Choi and Zhu [19] enhanced this approach by separating a toolpath set into individual toolpaths. They [20] further developed a dynamic priority-based approach for concurrent multi-material deposition based on the decoupled method in multi-object motion planning. However, their methods were developed based on mobile robots, and more operational constraints should be considered to handle practical mechanisms and ensure process safety.

In recent years, robotic arms or actuators have been introduced to develop vector-based AM systems [21-24]. In comparison with the traditional X-Y-Z stage mechanism, robotic actuators seem more flexible for vector-based AM. They offer larger work envelopes and facilitate realization of hybrid process and multi-actuator collaboration.

Indeed, robotic arms have long been used for collaborative manufacturing, like welding and product assembly. Toolpath planning for collision avoidance and efficiency improvement has been extensively studied for these applications [25-29]. However, toolpath planning for multiple robotic actuators in AM is significantly different, and the current methods cannot be used directly. It should not be presumed that toolpath planning of 2.5D actuator motion for AM may be simpler than 3D motion for non-AM applications. Firstly, the actuator motion for non-AM is mostly fixed for a particular job which can be defined with a few critical positions, such as the start and end points and some mid-points. But in AM, the toolpaths are determined by many layer contours of significantly varying shapes and layouts. As such, the toolpaths for non-AM are generally repetitive and pre-programmable by human operators, while those for AM vary considerably from layer to layer which can only be practically processed by complex algorithms with sufficient intelligence. Secondly, robotic actuators are usually used for pick-and-place tasks in non-AM applications without much consideration of tool velocities; in contrast, AM tools have to follow specific deposition paths and velocities determined mostly by material properties to ensure fabrication quality. Thirdly, it is necessary to consider material deposition priorities in AM. Some materials may have to be deposited prior to others for various quality reasons like strength, thermal shrinkage and warpage. However, robotic actuators for sequential tasks in non-AM applications are often pre-programmed to strictly follow some fixed sequences with little of the flexibility essential for AM. In summary, toolpath planning of robotic actuators for AM is different from and somewhat more complicated than for non-AM applications, and it remains a critical issue to be addressed.

This paper therefore proposes a deposition group-based approach for toolpath planning of MMAM with multiple robotic actuators. Operational spatial constraints of possible collisions between robotic actuators are classified as distance-, position- and region-based and modelled accordingly. Layer contours are sorted according to three criteria of collision avoidance, material deposition priorities, and material distribution on the actuators. The contour areas eligible for concurrent deposition are arranged into a deposition group. While the groups in a layer are processed sequentially one by one, the contours inside each group are deposited concurrently by multiple actuators. To exploit multiple robotic actuators for fabrication of relatively large single-material objects, the approach is extended by introducing three practical criteria to assign appropriate actuators carrying identical material to specific contour areas, and adjusting the sorting procedures accordingly. As such, the approach facilitates fabrication of complex multi-material objects, as well as large single-material objects, by reducing the build time considerably while ensuring process safety.

2. Spatial constraints of multiple robotic actuators

We now study the characteristics and modeling of three main operational spatial constraints of multiple robotic actuators, as well as indexing of material deposition priorities. Let's examine a layer of a sample multi-material part sliced by an X-Y slice plane in Fig. 1. It contains some outer contours (C1, C3, C4, C5 and C6) and inner contours (C2 and C7). A contour family (*CF*), formed by an outer contour together with the inner contour(s) inside it, if any, defines a solid area for deposition by a specific material [30]. There are six *CF*s to be deposited by multiple robotic actuators carrying four materials. Fabrication efficiency can be improved by concurrent deposition of the *CF*s with their corresponding actuators. However, whether two *CF*s can be deposited concurrently depends on factors likes the types and layout of the actuators, the materials carried by each actuator, the deposition priorities, and potential collisions between the actuators. It is essential to model various operational spatial constraints of the actuators.

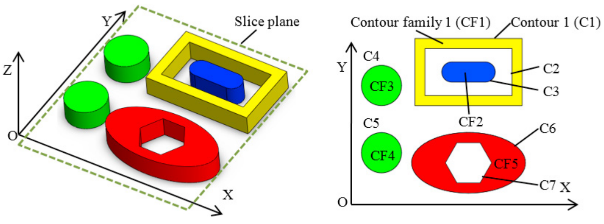

(a) CAD model of the sample part (b) A layer showing contour relationships

Fig. 1. A sample multi-material part and the contours within a layer.

2.1. Distance-based spatial constraint

Let's consider depositing two *CF*s by two actuators concurrently. Whether this is possible depends primarily on the distance between the two *CF*s. If they are too close, there may be collisions between the end-effectors. This constraint can be modelled by assigning to each *CF* a safety envelope based on the end-effector radius, as in Fig. 2(a); envelope overlap tests are then conducted to plan the deposition sequence [18]. As such, *CF*1 and *CF*2 can be deposited concurrently if their envelopes do not overlap. We extend this model not only for a series of independent nozzles, but also for end-effectors that each can deposit a number of materials, as in Fig. 2(b).

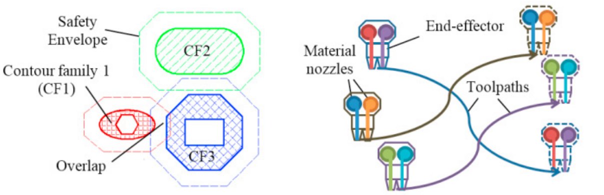

(a) Safety envelopes of contour families (b) End-effectors for multiple materials

Fig. 2. Modeling of distance-based spatial constraint

2.2. Region-based spatial constraint

In practical operations, collisions may take place not only between the end-effectors, but also between the link arms of the actuators and between the end-effectors and the link arms. This problem may exacerbate for selective compliance assembly robotic arms (SCARAs) or actuators with complicated link arm postures. Therefore, a constraint model based on division of sub-regions is developed to avoid such collisions.

In this model, each *CF* is given a safety envelope with an offset distance determined by the sizes of the end-effectors and link arms. For simplicity, rectangle envelopes are adopted. Eight open sub-regions are then constructed outside the envelope along the four edges, each of which is given an ID, as shown from R1 to R8 in Fig. 3(a). According to the posture and position of a *CF*'s corresponding actuator, one or more sub-regions are set to be the work region(s). To avoid collisions, any *CF*s located in these regions are not deposited concurrently with the central *CF*. In the example above, R7 is the work region for the blue *CF* because its corresponding robotic arm occupies part of this sub-region during deposition, as shown in Fig. 3(b). Since the red *CF* to be deposited by another actuator lies in R7, these two *CF*s cannot be deposited concurrently. In another example shown in Fig. 4(c), the work regions for the blue *CF* could be R5, R6 and R7 when it is deposited by a SCARA.

Based on this model, for two *CF*s, *CF*1 and *CF*2, they are firstly given safety envelops and work regions. Subsequently, interference of work regions, i.e., whether *CF*1 lies in any work region of *CF*2 or vice versa, will be checked. These two *CF*s can be deposited concurrently if there is no interference.

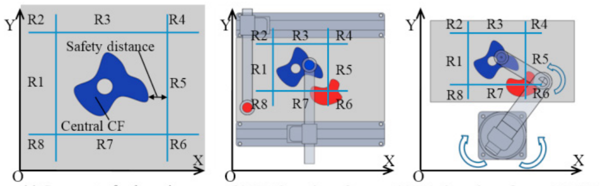

(a) Segment of sub-regions (b) Work regions for a Cartesian robotic arm (c) Work regions for an SCARA

Fig. 3. Modeling of region-based constraint.

2.3. Position-based spatial constraint

Position-based spatial constraint exists when the actuators have to follow a position order. A typical example is the composite X-Y stage with multiple actuators. In Fig. 5(a), each end-effector (actuator) can move independently, but they must follow a position order in the X-axis and cannot get across one another.

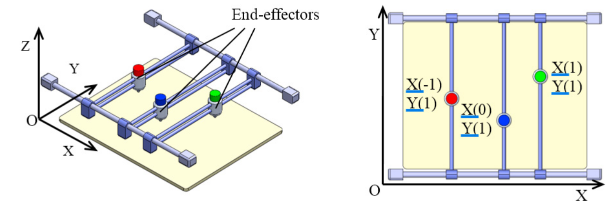

(a) Composite X-Y stage with 3 end-effectors (b) X- and Y- position indices for the end-effectors

Fig. 4. Modeling of position-based spatial constraint.

In a typical coordinate system, layers of fabrication materials are deposited in the X-Y plane and stacked along the Z-axis. To model position-based spatial constraint, each actuator is given a position index to indicate its order in the X- and Y-axis. A larger X index value indicates the actuator is on the right side of those with smaller values in the X-axis, and a larger Y index indicates it is above those with smaller values in the Y-axis. For the composite X-Y stage in Fig. 4(a), the three end-effectors can be given position indices X(-1), X(0), and X(1) to indicate their position order in the X-axis respectively. Since they do not have a restricted position order in the Y-axis, their indices are all set to be Y(0), as in Fig. 4(b).

Based on this model, for two *CF*s, *CF*1 and *CF*2, the proposed approach will check whether the positions of *CF*1 and *CF*2 match the position indices of their actuators. Specifically, it examines whether the *CF* whose actuator has a larger X index is located on the right side in X-axis, and that with a larger Y index is on the upper side in Y-axis. For example, if the X index of *CF*1's corresponding actuator is larger than that of *CF*2's, it means *CF*1's actuator should be on the right of *CF*2's. Therefore, if *CF*1 is located on the left of *CF*2, these two *CF*s cannot be deposited concurrently.

2.4. Material deposition priorities

The properties of materials for multi-material objects may vary significantly. To ensure fabrication quality, some materials may have to be deposited in a specific order or prior to others. This is vital for fabrication of cell-seeded biomedical scaffolds in tissue engineering, where certain materials have to be deposited first to construct scaffolds before living cells are placed. To model material property constraint, a priority index is assigned to each of the materials of an object to indicate the deposition priority of the related *CF*s. A material with a smaller priority index indicates that its *CF*s should be deposited before those of other materials with larger indices. For example, the *CF*s of a material with priority index (1) should be deposited prior to those of all other materials, and the *CF*s of a material with index (2) should be fabricated before those of another material with index (4).

2.5. Management of contour data

After slicing, sorting, and hatching operations [18], the contour data of an object are arranged according to their topological relationships into a hierarchical structure in Fig. 5 to facilitate subsequent toolpath planning. An entity in a higher hierarchy may consist of a number of entities of the adjacent lower hierarchy. For example, a layer may have to be deposited by several materials, each of which is assigned a unique RGB value.

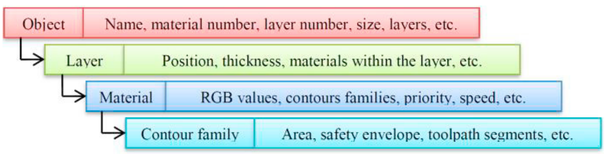

Fig. 5. Hierarchical structure for management of contour data

2.6. Operational data structure of actuators

The operational data of an actuator are structured as a comprehensive descriptor, as shown in Fig. 6. The geometrical data store the main dimensions of the actuator, including the length of a screw lead and the diameter of the end-effector. The position data indicate the actuator's position and posture during fabrication. The material data contain the RGB values of the materials on the end-effector. In previous works [8,9], the end-effector of an actuator can generally deposit at most four kinds of materials, which can satisfy most common applications while avoiding clumsiness of the deposition mechanism. This restriction is followed in this paper. The constraint data specify the operational spatial constraints of the actuators, such as X- and Y-position indices. The actuator ID is used in the sorting procedures to be presented below, where each layer CF would be assigned such an ID to indicate which actuator would deposit it.

With the data structure above, the relation between a multi-material object and the actuators can be established. By matching the RGB information in the object and the actuators, we can identify which actuator will deposit the CFs of a specific material. Moreover, the constraint data, position data, and ID of an actuator can be associated with the corresponding CFs with the same material for subsequent sorting. Using multiple actuators can also improve fabrication efficiency of large single-material objects by replacing the materials on their end-effectors with a single material for concurrent deposition of the object. However, the relation between the single-material object and the actuators cannot be determined with the data structure above, for the RGB data of all the actuators are the same. This will be dealt with in Section 4.

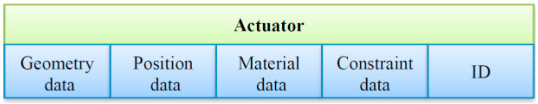

Fig. 6. Operational data structure of an actuator

3. Toolpath planning for MMAM

Fig. 7 shows the data structure for representing a multi-material object. An *Object* may be composed of a number of layers of materials (*Layers*), which form an array of layers (*LayerArray*). A *Layer* may contain several fabrication materials (*Materials*), which form an array of materials (*MaterialArray*). A *Material* may comprise some Contour families (*CFs*) forming a *CFArray*. Each *CF* is assigned an index Status to indicate its sorting status. Status 1 means the *CF* has been sorted, and 0 otherwise.

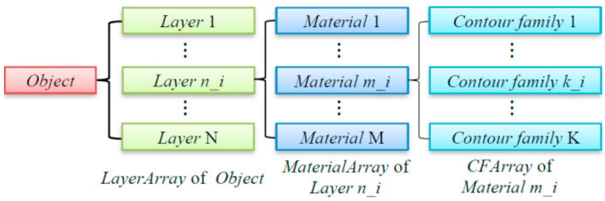

Fig. 7. Data representation of a multi-material object.

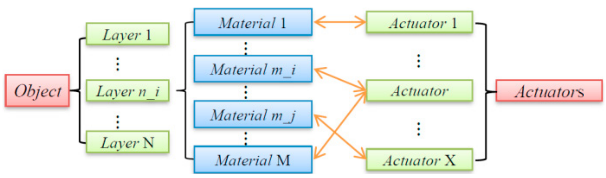

Fig. 8. Relationship between a multi-material object and the actuators.

We assume that deposition of a *CF* is completed in a one-off manner without pauses or disturbances. This ensures better fabrication quality and makes the toolpaths more practicable. Based on the relationship between an object and the actuators in Fig. 8, the following procedure elaborates the generation of concurrent toolpaths for the *CF*s in a specific layer.

Step 1: For each *CF* in the Layer, set Status=0 and associate the ID and the relevant position and constraint data of their corresponding Actuator with them respectively after matching the RGB information of the *Materials* they belong to and the *Actuators*.

Step 2: For the *CFArray* of each Material in the Layer, rearrange the order of *CF*s in them respectively by the deposition durations of the *CF*s.

Step 3: Rearrange the order of the Materials in the MaterialArray so that those with higher priorities will be listed ahead.

Step 4: For the first Material in the MaterialArray, pick up the first *CF* with Status=0 in its *CFArray*. Set the Status of this *CF* to be 1, and add it into the *ReadyArray*, which contains the *CF*s to be deposited in a group. If none of the *CF*s in the *CFArray* of this *Material* satisfy Status=0, try to pick up such a *CF* in the remaining *Materials* in priority order until one is found.

Step 5: For the remaining *Materials* in the MaterialArray, each *CF* in their individual *CFArray* with Status=0 will sequentially conduct the test shown in Fig. 9 with the *CF*(s) in the *ReadyArray*. For a *CF*, if the index *ToAdd* remains "True" after the test, it will be added into the *ReadyArray* and should be considered in the tests for remaining *CF*s. Meanwhile, the tests for the rest *CF*s in the current *CFArray* will be suspended, and the tests for the *CF*s in the *CFArray* of the next *Material* will begin.

Step 6: For all the *CF*s in the *ReadyArray*, set Status=1. These *CF*s will form a new deposition group to be deposited concurrently.

Step 7: Clear the *CF*(s) in the *ReadyArray*.

Step 8: If all the *CF*s in this *Layer* satisfy Status=1, continue sorting for the next *Layer*. Otherwise, return to Step 4, and repeat the rest steps for another deposition group.

Definitions:
TestCF: a *CF* in the *CFArray* to conduct test;
RefCF: a *CF* in the *ReadyArray*;
ToAdd: an index of whether to add the *TestCF* into the *ReadyArray*.

```
For each RefCF in the ReadyArray, check the following:
  if ( envelopes of TestCF and RefCF overlap ||
       material priority of TestCF < material priority of RefCF ||
       actuators of TestCF and RefCF are the same ||
       TestCF and RefCF interfere with each other's work regions ||
       positions of TestCF and RefCF violate the position indices of their actuators )
     set ToAdd = False;
  else
     set ToAdd = True;
```

Fig. 9. Tests to determine concurrent deposition of contour families

It should be noted that in Fig. 9, besides the tests for the constraints based on distance, work region, position and material priorities, an additional test is conducted to check whether *TestCF* and *RefCF* are the same one on the same actuator. Two *CF*s on the same actuator cannot be fabricated in the same deposition group.

The output of the sorting procedure above is shown in Fig. 10, which has taken collision avoidance, allocation of materials on actuators, and material deposition priorities into consideration. Each layer of an object would have one or more deposition groups, each consisting of one or more *CF*s to be deposited with different materials concurrently.

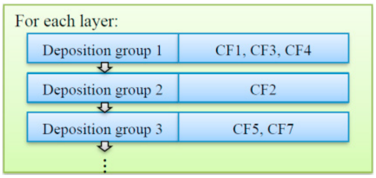

Fig. 10. Deposition groups in a layer

Different internal contour filling styles, either zigzag or spiral, will not affect the number and the constituent *CF*s of the deposition groups, because the sequencing operation is based on the safety envelopes of *CF*s. The data of the *CF*s within a deposition group are used to calculate the duration and end time of the group, and to determine the start time of the next group. In comparison with the previous works, the proposed algorithm sorts deposition sequence at *CF* level, instead of at material level. In other words, deposition of specific *CF*s may start earlier before finishing all the *CF*s of another material.

4. Extension of the toolpath planning algorithm for single-material objects

Single-material objects are preferable for cost-saving. However, most current vector-based AM systems are slow for fabricating large objects. It would be beneficial to extend the proposed algorithm to take advantage of multi-actuator MMAM systems for fabrication of large single-material objects.

4.1. Assignment of actuators for contours with identical material

A multi-actuator MMAM system should preferably be reconfigurable with relative ease for fabrication of single-material objects. From a hardware perspective, what an operator needs to do is, for example, to set the end-effectors to deposit identical material by attaching nozzles of the same material. However, from a toolpath-planning perspective, reconfiguring the system subjects all *CF*s in a layer to a one-to-multiple mapping on actuators, i.e., a *CF* can be deposited by any one of the actuators. This necessitates determining which actuator could better fabricate a specific *CF*. Three criteria are therefore proposed for assigning a specific *CF* to an appropriate actuator.

First, a *CF* should be within the work envelope of the actuator being assigned. This is because a contour should be deposited in a one-off manner, and an actuator is not able to fabricate a *CF* out of its reach. This criterion may exclude several actuators when fabricating a specific *CF* in a layer of a relatively large single-material object.

The other two criteria are based on the idle positions of actuators. We assign an idle position to each actuator to indicate where its end-effector rests when it is not depositing. Such an idle position is common for tools in machining centers and robotic arms in welding and assembly lines. In AM applications, an actuator's idle position is usually located at where the projections of its end-effector and the link structures are outside the area of a part. In toolpath planning for multi-material objects, it is not necessary to introduce such idle positions because the deposition relationship between *CF*s and actuators are already established, and they can be considered to be located at any place meeting the requirement above. However, idle positions are important considerations for actuator selection in single-material cases.

In the second criterion, during the deposition of a *CF* being analyzed, an actuator should not interfere with any other actuators that have not been assigned to work in the same deposition group. Specifically, the safety envelope and work regions, if any, of the *CF* should not overlap with the end-effectors and link structures of any other idle actuators. This criterion prevents actuators from colliding even when they are not depositing concurrently.

In the third criterion, the *CF* being analyzed will be enveloped into the smallest rectangle possible, and the distances between the center of this rectangle and the idle positions of the remaining actuators after the first two criteria will be calculated, respectively. The idle actuator nearest to this center will be assigned to fabricate this *CF*.

4.2. Toolpath planning for single-material objects

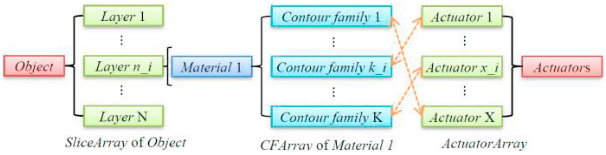

Fig. 11. Relationship between a single-material object and multiple actuators

According to the relationship between a single-material object and multiple actuators, as shown in Fig. 11, the following procedure is adopted to generate concurrent toolpaths for the *CF*s in a layer. Besides the previous index Status, a new index, *IsUsed*, is assigned to each Actuator to indicate whether it will deposit in a deposition group.

Step 1: For each *CF* within the Layer, set Status=0; for each Actuator in the *ActuatorArray*, set *IsUsed*=0.

Step 2: Rearrange the order of the *CF*s in the *CFArray* of the only Material according to the deposition durations of the *CF*s.

Step 3: For the first *CF* in the *CFArray* with Status=0, set Status=1, add it into the *ReadyArray*. Assign the ID, relevant constraint and position data of the first qualified Actuator in the *ActuatorArray* to this *CF*, and set *IsUsed*=1 for this Actuator. An Actuator is considered qualified if it satisfies the aforementioned three criteria.

Step 4: For each of the rest of *CF*(s) in the *CFArray* with Status=0, sequentially assign the ID and relevant data of all the Actuators in the *ActuatorArray* with *IsUsed*=0, and conduct the tests shown in Fig. 12 after each assignment. For a *CF*, if the *ToAdd* remains "True" in the tests after a certain assignment and the current Actuator is qualified, it will be added into the *ReadyArray*, and the selected Actuator will be set *IsUsed*=1. If all the Actuators have *IsUsed*=1, the tests for the rest *CF*(s) will be suspended.

Step 5: For all the *CF*s in the *ReadyArray*, set Status=1. These *CF*s will form a new deposition group to be deposited concurrently.

Step 6: Clear the *CF*(s) in the *ReadyArray*; for all the Actuators in the *ActuatorArray*, set *IsUsed*=0.

Step 7: If all the *CF*s in the Layer satisfy Status=1, continue to sort the next Layer. Otherwise, return to Step 3, and repeat the rest steps for another deposition group.

The output for each layer is a list of deposition groups, each of which may contain a number of *CF*s to be deposited concurrently with the same material. The calculation of start time, duration and end time of each *CF* is similar with that in multi-material objects.

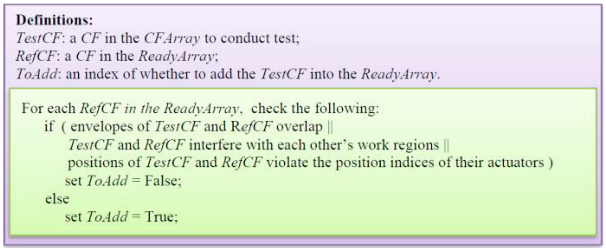
Definitions:
TestCF: a *CF* in the *CFArray* to conduct test;
RefCF: a *CF* in the *ReadyArray*;
ToAdd: an index of whether to add the *TestCF* into the *ReadyArray*.

```
For each RefCF in the ReadyArray, check the following:
    if ( envelopes of TestCF and RefCF overlap ||
         TestCF and RefCF interfere with each other's work regions ||
         positions of TestCF and RefCF violate the position indices of their actuators )
         set ToAdd = False;
    else
         set ToAdd = True;
```

Fig. 12. Tests for concurrent deposition of contour families of a single material.

5. Case studies

The proposed toolpath planning approach has been implemented in a virtual prototyping system incorporated with a simulation module based on SolidWorks SDK, VB.net, C++ and OpenGL library. Using this system, an AM fabrication scenario can be built conveniently, with the required object and actuator data extracted automatically and managed hierarchically. The resulting toolpaths and subsequent digital fabrication process can be visualized and validated. The following case studies demonstrate the proposed toolpath planning approach. For ease of comparison, the deposition speeds of all materials are set to be 30 mm/s, and the zigzag-style contour filling style is adopted.

5.1. A multi-material brooch

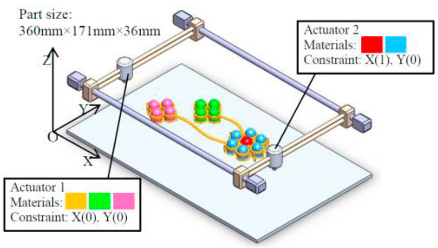

Fig. 13. A composite X-Y stage AM system with two actuators for fabrication of a multi-material brooch

Fig. 13 shows a composite X-Y stage AM system consisting of two actuators for fabrication of a multi-material brooch. A total of five materials are assigned to the end-effectors according to their distribution in the brooch. Since the brooch skeleton is made of orange material, it is assigned the highest deposition priority. The color STL model of the brooch is sliced into 100 layers with a hatch width of 1mm. The position-based spatial constraint between the two actuators is as follows. Actuator 1 is assigned X(0) and Y(0) as its X- and Y-position index, respectively, while Actuator 2 is X(1) and Y(0). Moreover, a safety distance of 20mm is assigned to each actuator according to the dimensions of their end-effectors.

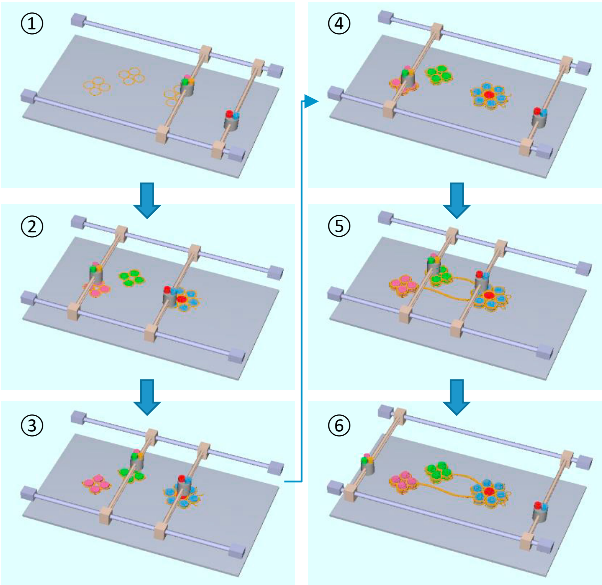

Fig. 14. Digital fabrication of the brooch.

Based on the settings above, concurrent toolpaths are generated for subsequent digital fabrication, several stages of which are shown in Fig. 14. To illustrate some toolpaths in detail, a layer of the brooch is selected. Fig. 15 highlights the *CF*s with their safety envelopes, and the digital fabrication process based on these toolpaths is shown in Fig. 16.

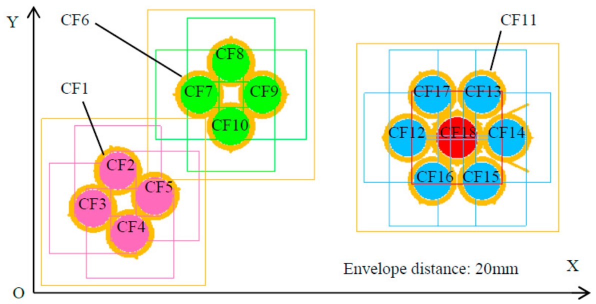

Fig. 15. A selected brooch layer.

It can be seen that the orange material is deposited first, as defined by the material priority. It can also be seen that, except for some *CF*s which are inevitably deposited sequentially, the two actuators are capable of depositing the remaining *CF*s concurrently. The total build time for this brooch is about 345.58 minutes with the concurrent toolpaths generated by the proposed approach. In comparison, it takes 543.78 minutes with sequential toolpaths, 399.50 minutes with the envelope-based approach [18] and 328.19 minutes with the dynamic priority-based approach [20]. It should be pointed out that the other two methods were developed based on independent mobile robots which had only distance constraints and do not exist yet, while the proposed method uses the more realistic X-Y table mechanism. This shows that the proposed approach, with more realistic spatial constraint modelling and fewer independent actuators, compares favorably with the current methods, which virtually over-simplify or consider very few operational constraints.

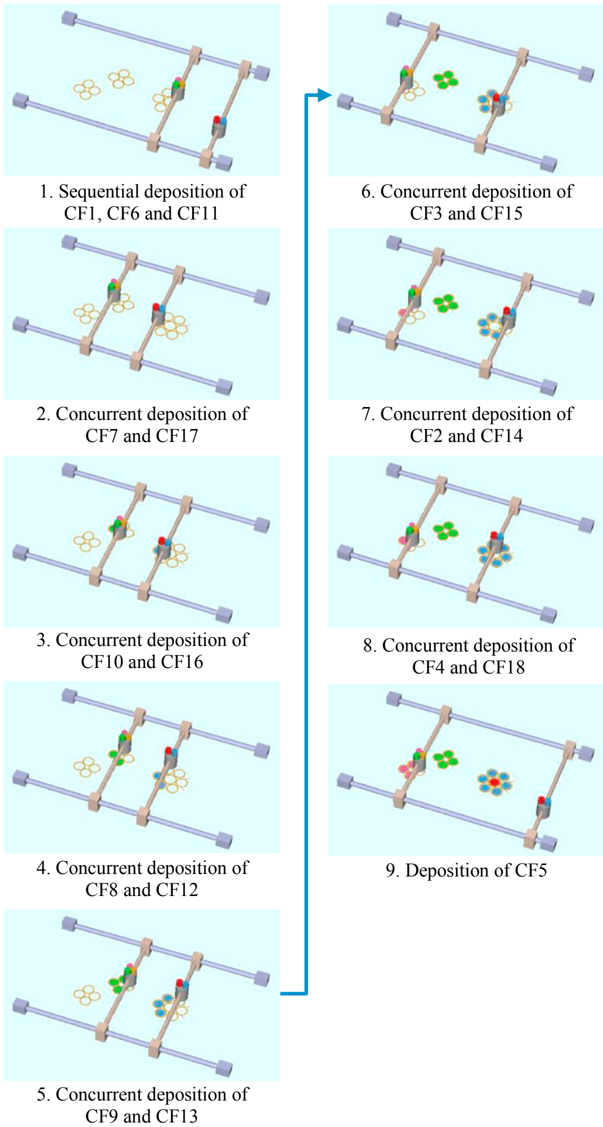

Fig. 16. Digital fabrication of the selected brooch layer with concurrent toolpaths.

5.2. A fixture

In manufacturing, fixtures are often used for securing workpieces. A possible application of AM is to fabricate customer-specific fixtures. Fig. 17 shows an AM system consisting of two Cartesian robotic arm actuators for fabrication of a fixture of eight materials. The color STL model of the fixture model is sliced into 250 layers, and the hatch width for internal filling of the *CF*s is 1mm. According to their distribution, the eight materials are assigned to the two robotic arms. To model the region-based constraint, R7 and R3 are set as the work regions for these two actuators respectively. Moreover, a 20mm safety distance is assigned to each robotic arm according to the dimensions of their end-effectors. After generating concurrent toolpaths, the multi-material fixture can be digitally fabricated and visualized, as shown in Fig. 18. The total build time is about 12.05 hours with the concurrent toolpaths, and 13.26 hours with sequential toolpaths.

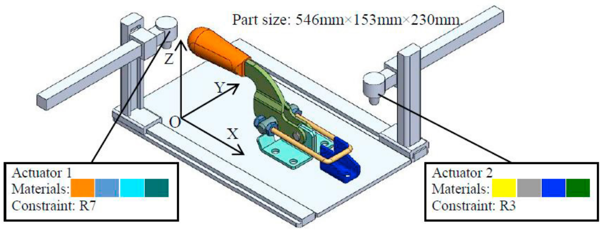

Fig. 17. An AM system with two robotic arm actuators for fabrication of a multi-material fixture

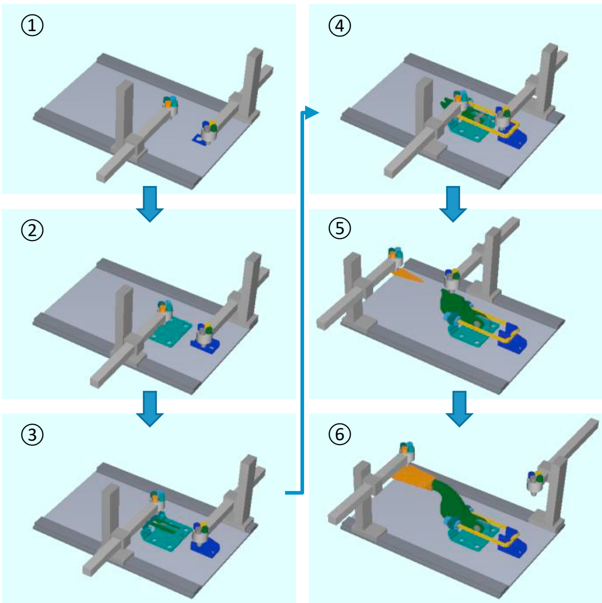

Fig. 18. Digital fabrication of the multi-material fixture

For some applications, a single-material fixture may be good enough and cost-effective. In this case, a monochrome STL model of the fixture can be loaded, as shown in Fig. 19. The region-based constraint, the slicing parameters and the hatch width are the same as before. The total build time of the single-material fixture is about 11.82 hours with concurrent toolpaths, and about 13.26 hours in a traditional AM system with only one actuator. To illustrate the concurrent toolpaths, a layer of the single-material fixture model is selected. Fig. 20 shows the *CF*s with their safety envelopes, while Table 2 shows the deposition groups and the toolpath sequence for this layer. Digital fabrication of this layer based on the toolpaths is shown in Fig. 21. It can be seen that although some *CF*s are inevitably deposited sequentially, the two actuators deposit the remaining contours concurrently.

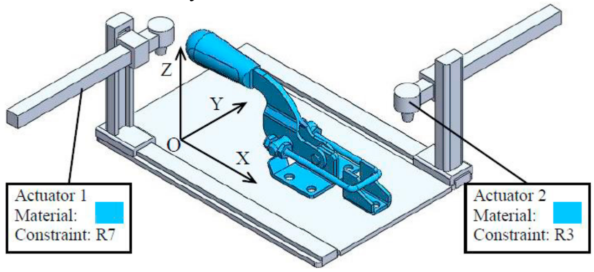

Fig. 19. An AM system with two robotic arm actuators for fabrication of a single-material fixture.

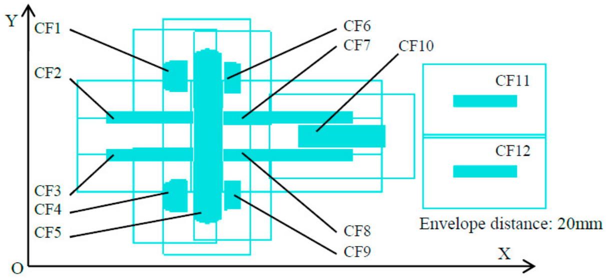

Fig. 20. A selected layer of the single material fixture.

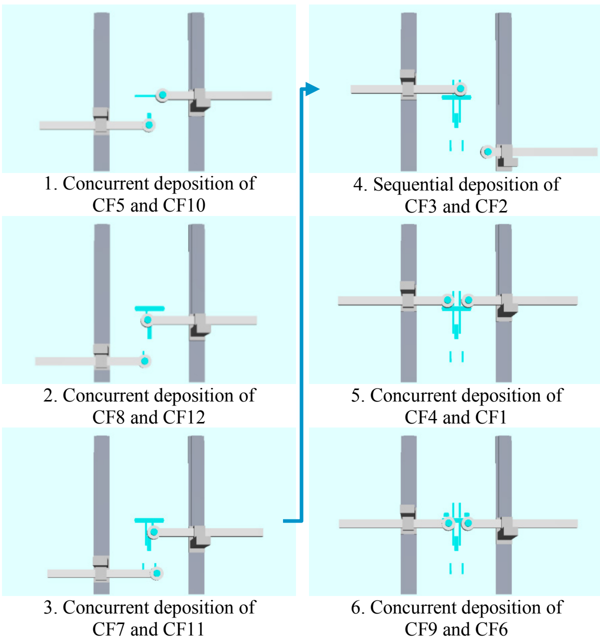

Fig. 21. Digital fabrication of the selected fixture layer with concurrent toolpaths.

5.3. Contour crafting of a single-material cottage

Contour crafting [31] is a large-scale AM process with multi-gantry configuration to construct a building layer by layer. Fig. 20 shows the construction of a single-material cottage by two gantry-style actuators, modelled with the position-based constraint. The rooftop has been set transparent for visualization of internal structures. Fig. 23(a) presents a cottage layer sliced with an X-Y plane. The cross section is a single *CF* because the walls are inter-connected, but it can be divided into edge segments at the wall intersections to speed up fabrication [31], as in Fig. 23(b). The safety envelopes are based on the sizes of the end-effectors of the gantries, as in Fig. 23(c). The total build time is about 39.64 hours with the concurrent toolpaths, and 59.61 hours with sequential toolpaths.

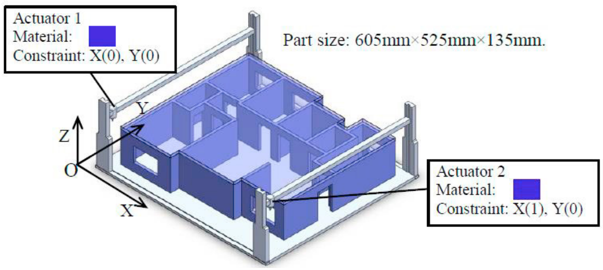

Fig. 22. An AM system with two gantries for contour crafting of a cottage.

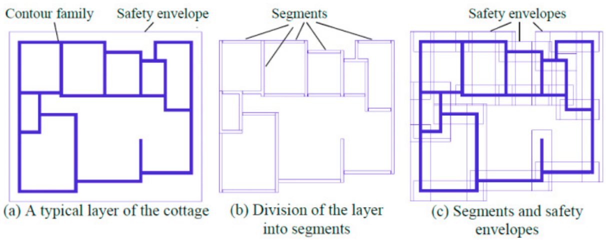

Fig. 23. Processing of layer contours of the cottage.

4. Conclusions

This paper presents a practical toolpath planning approach, based on deposition groups for concurrent deposition by multiple actuators, to improve fabrication efficiency of both multi-material and single-material objects. The operational spatial constraints causing actuator collisions are classified and modelled, and material deposition priorities are indexed. The layer contours are sorted based on actuator collision avoidance, material deposition priorities, and material distribution on the actuators. The contours eligible for concurrent deposition are arranged into a series of deposition groups, within each of which all the contours will be deposited concurrently. This approach is extended to improve fabrication efficiency of relatively large single-material objects, by adjusting the sorting procedures based on three criteria to determine an appropriate actuator for a specific contour family. The proposed approach has been implemented in a virtual prototyping system for simulation and visualization of MMAM processes. Case studies show that it can effectively consider operational spatial constraints to avoid collisions and uphold material deposition priorities to ensure fabrication quality. This exploits the potential of multiple robotic actuators to improve fabrication efficiency of both multi- and single-material objects. It can indeed be adapted for control of physical MMAM processes.

At the current stage, the proposed approach employs rectangular safety envelopes and eight sub-regions for constraint modeling. Indeed, if appropriate envelopes other than rectangles or more sub-regions are adopted, more efficient toolpaths can be generated. Moreover, during their individual deposition, the *CF*s of a specific actuator can have different work regions according to the diverse postures of the actuator. However, such strategies would inevitably incur much computation burden for posture and interference calculations, although they are worthy of future development.

Acknowledgements

The authors would like to acknowledge the CRCG of the University of Hong Kong for its financial support for this project.

References

[1] N. Hopkinson, R. Hague and P. Dickens 2006. Emerging rapid manufacturing processes. In: Hopkinson, N., et al. (eds.) Rapid manufacturing: an industrial revolution for the digital age. John Wiley & Sons.

[2] W. Cho, E. Sachs, N. Patrikalakis and D. Troxel, A dithering algorithm for local composition control with three-dimensional printing. Computer-Aided Design, 2003; 35(9): 851-867.

[3] V. Beal, P. Erasenthiran, N. Hopkinson, P. Dickens and C. Ahrens, Fabrication of x-graded H13 and Cu powder mix using high power pulsed Nd: YAG laser. In Proceedings of Solid Freeform Fabrication symposium, 2004, 187-197.

[4] H. Kim, J. W. Choi and R. Wicker, Scheduling and process planning for multiple material stereolithography. Rapid Prototyping Journal, 2010; 16(4): 232-240.

[5] W. Han, M. Jafari and K. Seyed, Process speeding up via deposition planning in fused deposition-based layered manufacturing processes. Rapid Prototyping Journal, 2003; 9(4): 212-218.

[6] K.-H. Shin, H. Natu, D. Dutta and J. Mazumder, A method for the design and fabrication of heterogeneous objects. Materials & Design, 2003; 24(5): 339-353.

[7] E. C. Santos, M. Shiomi, K. Osakada and T. Laoui, Rapid manufacturing of metal components by laser forming. International Journal of Machine Tools and Manufacture, 2006; 46(12-13): 1459-1468.

[8] S. Khalil and W. Sun, Biopolymer deposition for freeform fabrication of hydrogel tissue constructs. Materials Science and Engineering: C, 2007; 27(3): 469-478.

[9] L. Li, M. Saedan, W. Feng, J. Fuh, Y. Wong, H. Loh, S. Thian, S. Thoroddsen and L. Lu, Development of a multi-nozzle drop-on-demand system for multi-material dispensing. Journal of Materials Processing Technology, 2009; 209(9): 4444-4448.

[10] DMD. 2018. http://www.pomgroup.com/

[11] Optomec. 2018. http://www.optomec.com/

[12] A. Bellini.2002. Fused deposition of ceramics: a comprehensive experimental, analytical and computational study of material behavior, fabrication process and equipment design. Ph.D, Drexel University.

[13] J. Giannatsis and V. Dedoussis, Additive fabrication technologies applied to medicine and health care: a review. The International Journal of Advanced Manufacturing Technology, 2009; 40(1): 116-127.

[14] T. Wohlers, Wohlers Report 2015. State of the industry, Annual worldwide progress report, Wohlers Associates Inc., United State of America, 2015.

[15] J. Wachsmuth.2008. Multiple Independent Extrusion Heads for Fused Deposition Modeling. Master of Science, Virginia Polytechnic Institute and State University.
[16] J. Zhang and B. Khoshnevis, Contour Crafting Process Plan Optimization Part II: Multi–Machine Cases. 2010.
[17] W. Zhu and K. Yu, Tool path generation of multi-material assembly for rapid manufacture. Rapid Prototyping Journal, 2002; 8(5): 277-283.
[18] S. H. Choi and H. H. Cheung, A topological hierarchy-based approach to toolpath planning for multi-material layered manufacturing. Computer-Aided Design, 2006; 38(2): 143-156.
[19] S. H. Choi and W. K. Zhu, Efficient concurrent toolpath planning for multi-material layered manufacturing. In Proceedings of Solid Freeform Fabrication Symposium, 2009, 429-440.
[20] S. H. Choi and W. K. Zhu, A dynamic priority-based approach to concurrent toolpath planning for multi-material layered manufacturing. Computer-Aided Design, 2010; 42(12): 1095-1107.
[21] E. Barnett, J. Angeles, D. Pasini and P. Sijpkes, Robot-assisted Rapid Prototyping for ice structures. In Proceedings of Robotics and Automation, 2009. ICRA '09. IEEE International Conference on, 2009, 146-151.
[22] J. G. Dellinger, J. Cesarano and R. D. Jamison, Robotic deposition of model hydroxyapatite scaffolds with multiple architectures and multiscale porosity for bone tissue engineering. Journal of Biomedical Materials Research Part A, 2007; 82A(2): 383-394.
[23] A. Djuric and J. Urbanic, Design and evaluation of reconfigurable robotic systems for 2 1/2 axis based material deposition strategies. Integrated Computer-Aided Engineering, 2009; 16(4): 315-338.
[24] R. Dwivedi and R. Kovacevic, Morphing based approach for process planning for fabrication of geometries and the control of material composition. In Proceedings of Solid Freeform Fabrication Symposium, 2004, 553-562.
[25] S. Akella and J. Peng, Time-scaled coordination of multiple manipulators. In Proceedings of 4, 2004, 3337-3344.
[26] M. Ali, N. Babu and K. Varghese, Collision Free Path Planning of Cooperative Crane Manipulators Using Genetic Algorithm. Journal of Computing in Civil Engineering, 2005; 19(2): 182-193.
[27] C. Chang, M. Chung and Z. Bien, Collision-free motion planning for two articulated robot arms using minimum distance functions. Robotica, 2009; 8(02): 137-144.
[28] J. Fraile, J. Perez-Turiel, J. Gonzalez-Sanchez, E. Baeyens and R. Perez, Comparative analysis of collision-free path-planning methods for multi-manipulator systems. Robotica, 2006; 24(06): 711-726.
[29] X. J. Wu, J. Tang, Q. Li and K. H. Heng, Development of a configuration space motion planner for robot in dynamic environment. Robotics and Computer-Integrated Manufacturing, 2009; 25(1): 13-31.
[30] S. H. Choi and H. H. Cheung, A multi-material virtual prototyping system. Computer-Aided Design, 2005; 37(1): 123-136.
[31] J. Zhang and B. Khoshnevis, Contour Crafting Process Plan Optimization Part I: Single-Nozzle Case. 2010.